Published in final edited form as:
J Magn Reson. 2011 June ; 210(2): 233–237. doi:10.1016/j.jmr.2011.03.012.

Effect of gradient pulse duration on MRI estimation of the diffusional kurtosis for a two-compartment exchange model

Jens H. Jensen[1,*] and **Joseph A. Helpern**[1]

[1] Department of Radiology, New York University School of Medicine, 660 First Avenue, New York, NY, 10016-3295, USA

Abstract

Hardware constraints typically require the use of extended gradient pulse durations for clinical applications of diffusion-weighted magnetic resonance imaging (DW-MRI), which can potentially influence the estimation of diffusion metrics. Prior studies have examined this effect for the apparent diffusion coefficient. This study employs a two-compartment exchange model in order to assess the gradient pulse duration sensitivity of the apparent diffusional kurtosis (ADK), a quantitative index of diffusional non-Gaussianity. An analytic expression is derived and numerically evaluated for parameter ranges relevant to DW-MRI of brain. It is found that the ADK differs from the true diffusional kurtosis by at most a few percent. This suggests that ADK estimates for brain may be robust with respect to changes in pulse gradient duration.

Keywords

Diffusion-weighted magnetic resonance imaging; Diffusional kurtosis; Pulse gradient duration; Kärger model; Brain

1. Introduction

Because of the limited gradient strengths available on human scanners, clinical applications of diffusion-weighted magnetic resonance imaging (DW-MRI) typically require the use of extended pulse durations for the diffusion-sensitizing gradients in order to obtain a sufficient degree of diffusion weighting [1]. As a consequence, apparent diffusion coefficient (ADC) estimates derived from clinical DW-MRI data may differ, in principle, from their ideal values as would be obtained in the narrow pulse limit. For closed geometries with impenetrable barriers, it has indeed been demonstrated that the diffusion-weighted NMR signal can be highly sensitive to the pulse duration [2]. However, for the more open geometries relevant to biological tissues, the effect of gradient pulse duration on ADC estimates is believed to be generally modest [3], supporting a view that clinical diffusivity maps are reasonably robust with respect to pulse duration changes.

Recently, it has been shown that the diffusional kurtosis, a measure of diffusional non-Gaussianity, can also be estimated with clinical DW-MRI [4–7]. Preliminary studies suggest

*Correspondence to: Jens H. Jensen, Department of Radiology, New York University School of Medicine, 660 First Avenue, 4th Floor, New York, NY 10016-3295. jj33@nyu.edu; Tel.: (212)263-6605; FAX: (212)263-7541.

that the diffusional kurtosis holds promise as a metric for characterizing neural tissue microstructure [8–12] and for studying pathologies such as tumors [13,14], ischemic stroke [15] and attention-deficit disorder [16]. Just as for the ADC, the apparent diffusional kurtosis (ADK) obtained with DW-MRI can potentially depend on the gradient pulse duration. Although one experiment has found the ADK in rat thalamus to be robust with respect to pulse duration changes [17], the pulse duration sensitivity of the ADK has not been previously addressed theoretically. In this article, we investigate the effect of pulse duration for a specific diffusion model that permits analytic solution.

The model we consider is the two-compartment version of the exchange model first proposed by Kärger and coworkers [18,19]. Although highly idealized, the Kärger model (KM) captures essential qualitative features of water diffusion in biological tissues, where the compartments plausibly represent intra- and extra-cellular spaces with differing compartmental diffusivities [20–23]. The exchange between compartments occurs via diffusion across the cell membranes. When the membrane permeability is sufficiently low, this transport can be accurately characterized by an exchange rate. Modifications of the KM have also been proposed [24,25] in order to better describe diffusion in certain types of tissues.

One special property of the KM is that the ADC is independent of the pulse duration, but this is largely consistent with empirical observations for water diffusion in brain [17]. The ADK for the KM does, in contrast, depend on the pulse duration, as we shall show explicitly for the case of two compartments. The magnitude of this dependence provides an indicator of the robustness of the ADK with respect to changes in gradient pulse duration and of how much the ADK may deviate from the true diffusional kurtosis.

2. Theory

2.1. Apparent diffusion metrics

The diffusion coefficient in a particular direction may be defined by

$$D(T) \equiv \frac{1}{2T}\langle x^2(T)\rangle, \tag{1}$$

where $x(T)$ is the net displacement of a diffusing spin over a time interval T and the angle brackets signify an averaging over all the spins within a region of interest (e.g., a voxel).

For pulsed gradient DW-MRI, the ADC measured with a signal readout time TE corresponds to

$$D_{\text{app}} \equiv \frac{\gamma^2}{2b}\int_0^{\text{TE}} dt_2 \int_0^{\text{TE}} dt_1 \sigma(t_1)\sigma(t_2)g(t_1)g(t_2)\langle x(t_1)x(t_2)\rangle, \tag{2}$$

where $g(t)$ gives the time dependence for the diffusion-sensitizing gradient pulse, b is the so-called b-value, $\sigma(t)$ is the spin flip function, and γ is the gyromagnetic ratio for the spins [4]. In Eq. (2), we assume that the initial radiofrequency excitation occurs at a time $t_0 = 0$ and that $x(t)$ represents, as in Eq. (1), the net displacement over a time interval t.

The b-value is given explicitly by

$$b \equiv 2\gamma^2 \int_0^{\mathrm{TE}} dt_2 \int_0^{t_2} dt_1 \sigma(t_1)\sigma(t_2)g(t_1)g(t_2)t_1, \tag{3}$$

while the spin flip function has unit magnitude and changes sign at times corresponding to any 180° radio frequency inversion pulses [26]. For the sake of simplicity, we have taken the gradients to be unidirectional and aligned with the diffusion direction of interest. The condition that the NMR signal be refocused requires that

$$0 = \int_0^{\mathrm{TE}} dt \sigma(t)g(t). \tag{4}$$

Note that Eqs. (2)–(3) imply that the ADC, as we have defined it, depends of the gradient time dependence but not on its strength (i.e., the ADC is invariant with respect to a rescaling of g). This definition of the ADC corresponds to minus the initial slope for the natural logarithm of NMR signal amplitude as a function of the b-value.

For the classic Stejskal-Tanner pulse sequence [27,28], the gradient pulse takes the form

$$\sigma(t)g(t) = g_0[H(t-\Delta) - H(\delta - t)], \tag{5}$$

for $0 \leq t \leq \Delta + \delta$ and with $H(t)$ being the Heaviside step function (outside this interval the gradient pulse vanishes). The gradient amplitude is parameterized by g_0, the pulse duration is δ, and the diffusion time is Δ. Consistency requires that $\Delta \geq \delta$.

By applying Eq. (5) to Eq. (3) and setting $\mathrm{TE} = \Delta + \delta$, one may readily verify the familiar expression

$$b = (\gamma g_0 \delta)^2 (\Delta - \delta/3). \tag{6}$$

Moreover, one can show

$$\lim_{\delta \to 0} D_{\mathrm{app}}(\Delta, \delta) = D(\Delta), \tag{7}$$

so that the ADC approaches the true diffusion coefficient in the narrow pulse limit.

The diffusional kurtosis is defined by [4,6]

$$K(T) \equiv \frac{\langle x^4(T) \rangle}{\langle x^2(T) \rangle^2} - 3. \tag{8}$$

For Gaussian diffusion, $K(T)$ vanishes and, more generally, it provides a dimensionless index of diffusional non-Gaussianity.

The ADK determined from DW-MRI data is given by [4]

$$K_{\mathrm{app}} \equiv \frac{\gamma^4}{(2bD_{\mathrm{app}})^2} \int_0^{\mathrm{TE}} dt_4 \int_0^{\mathrm{TE}} dt_3 \int_0^{\mathrm{TE}} dt_2 \int_0^{\mathrm{TE}} dt_1 \sigma(t_1)\sigma(t_2)\sigma(t_3)\sigma(t_4) g(t_1)g(t_2)g(t_3)g(t_4) \times [\langle x(t_1)x(t_2)x(t_3)x(t_4)\rangle - 3\langle x(t_1)x(t_2)\rangle\langle x(t_3)x(t_4)\rangle]. \quad (9)$$

In analogy with Eq. (7), we have, for the Stejskal-Tanner pulse sequence, the narrow pulse limit

$$\lim_{\delta \to 0} K_{\mathrm{app}}(\Delta, \delta) = K(\Delta). \quad (10)$$

As for the ADC, the ADK as defined by Eq. (9) is independent of the gradient strength.

2.2. Kärger model

The general KM is characterized by N compartments with intrinsic diffusivities D_i and relative particle number fractions f_i for i =1,2, …, N. The exchange between compartments is governed by the transition rate constants R_{ij} for a jump from compartment j to compartment i. For diffusion in the direction of the x coordinate, the basic KM equations are then [19]

$$\frac{\partial}{\partial t} C_i(x,t) = D_i \frac{\partial^2}{\partial x^2} C_i(x,t) + \sum_{j=1}^{N} R_{ij} C_j(x,t), \quad \text{for } i = 1, 2, \ldots, N, \quad (11)$$

where $C_i(x,t)$ is the particle concentration at position x and time t. The concentrations are related to the number fractions by

$$f_i = \int_{-\infty}^{\infty} dx C_i(x,t) \Big/ \sum_{j=1}^{N} \int_{-\infty}^{\infty} dx C_j(x,t). \quad (12)$$

By definition, the number fractions satisfy

$$1 = \sum_{i=1}^{N} f_i. \quad (13)$$

For the f_i to be independent of time requires also that

$$0 = \sum_{j=1}^{N} R_{ij} f_j. \quad (14)$$

In addition, detailed balance demands that [29]

$$R_{ji}f_i = R_{ij}f_j, \tag{15}$$

which follows from an assumption of time reversal symmetry in the underlying microscopic dynamics [30]. The equilibrium condition of Eq. (14) is explicitly stated by Kärger and coworkers [19]. While they do not mention the detailed balance condition of Eq. (15), it is generally appropriate for water diffusion in biological tissues and implicitly utilized in their analysis for the two-compartment case of $N = 2$ [18,19]. When $R_{ij} = 0$, Eq. (11) simply reduces to N independent diffusion equations for the concentrations C_i.

For the rate constants, we adopt the convention that R_{ij} is for a transition from j to i, rather than the i to j convention employed by Kärger et al. [19]. The j to i convention is often used in the context of master equations [29], which are the closely related to the KM, and has the advantage of being more consistent with the standard index notation used in linear algebra.

By taking into account the constraints of Eqs. (13)–(15), the N compartment KM is seen to be described by a total of $(N^2 + 3N - 2) / 2$ free parameters. We emphasize the equilibrium and detailed balance conditions are fully independent. In particular, Eq. (14) restricts the diagonal components of R_{ij}, but Eq. (15) does not.

For the special case of $N = 2$, which we now consider in detail, the four free parameters may be taken as the compartmental diffusivities D_1 and D_2, the number fraction $f_1 = 1 - f_2$, and the exchange rate constant $R_e \equiv R_{12} / f_1 = R_{21} / f_2$.

The second order position correlation function for the KM with $N = 2$ is

$$\langle x(t_1)x(t_2)\rangle = 2\bar{D}t_1, \tag{16}$$

assuming that $t_1 \leq t_2$, where $\bar{D}$ is the averaged diffusion coefficient for the total system given by

$$\bar{D} \equiv f_1 D_1 + f_2 D_2. \tag{17}$$

It should be noted that Eq. (16) covers the general case since for $t_1 > t_2$ one may simply use the trivial identity $x(t_1)x(t_2) = x(t_2)x(t_1)$ to find $\langle x(t_1)x(t_2)\rangle = 2\bar{D}t_2$. Since t_1 and t_2 refer to time intervals (i.e., time periods over which the diffusion is observed), Eq. (16) is consistent with time translation invariance, as is required for a stationary system. For $t_1 = t_2$, Eq. (16) is equivalent to the familiar expression of Eq. (1). The spatial averaging implied in Eq. (16) is elementary since the KM lacks geometrical structure. That the right side of Eq. (16) contains only a single time parameter is related to the fact that velocities for the KM are uncorrelated for different time intervals.

The fourth order position correlation function for the two-compartment KM is

$$\langle x(t_1)x(t_2)x(t_3)x(t_4)\rangle = 4\overline{D}^2 t_1(2t_2+t_3) + \frac{4\overline{D}^2 K_0}{3R_e^2}[6R_e t_1 + 3e^{-R_e t_1} + 2e^{-R_e t_2} + e^{-R_e t_3} - 2e^{-R_e(t_2-t_1)} - e^{-R_e(t_3-t_1)} - 3], \tag{18}$$

assuming that $t_1 \leq t_2 \leq t_3 \leq t_4$. The parameter K_0 corresponds to the initial diffusional kurtosis and is given explicitly by

$$K_0 \equiv 3 f_1 f_2 \frac{(D_1 - D_2)^2}{\overline{D}^2}. \tag{19}$$

Just as with Eq. (16), commutativity of the positions implies that the fourth order correlation function for an arbitrary time ordering can be derived from Eq. (18). The derivations of Eqs. (16) and (18) are outlined in the Appendix.

By using Eqs. (1), (8), (16), and (18), we find the two-compartment KM diffusion metrics:

$$D(T) = \overline{D}, \tag{20}$$

and

$$K(T) = \frac{2K_0}{R_e T}\left[1 - \frac{1}{R_e T}(1 - e^{-R_e T})\right]. \tag{21}$$

The KM kurtosis of Eq. (21) was derived first for $f_1 = f_2$ by Cao [31] and for arbitrary volume fractions by Jensen and co-workers [4]. Note that the kurtosis depends on the observation time interval and the exchange rate constant, but the diffusion coefficient is a constant and independent of the exchange rate constant as has been observed in several prior studies [6,20,21,23].

By performing the integrals in Eqs. (2) and (9) with TE = $\Delta + \delta$, the KM ADC and ADK for a Stejskal-Tanner sequence can be determined analytically as

$$D_{\text{app}}(\Delta, \delta) = \overline{D}, \tag{22}$$

and

$$K_{\text{app}}(\Delta, \delta) = \frac{2K_0}{15(X - Y/3)^2 Y^4}[15XY^4 - 9Y^5 - 40Y^3 + 60Y^2 - 120 + 120(Y+1)e^{-Y} + 120(Y-1)e^{-X} + 60(Y-1)^2 e^{-X+Y} + 60e^{-X-Y}], \tag{23}$$

with $X \equiv R_e\Delta$ and $Y \equiv R_e\delta$. So for the KM, the ADC is exactly equal to the true diffusion coefficient for any value of the gradient pulse duration. The ADK differs, in general, from the true kurtosis, but Eq. (23) is consistent with the narrow pulse limit of Eq. (10).

3. Results

In order to investigate the deviation of the KM ADK from the true kurtosis, we define the percent error as:

$$\varepsilon \equiv 100 \cdot \frac{K_{\text{app}}(\Delta, \delta) - K(\Delta)}{K(\Delta)}. \tag{24}$$

By using Eqs. (21) and (23), this error was calculated for $0 \leq \delta / \Delta \leq 1$and $0 \leq R_e \Delta \leq 10$. This includes the range of physical interest for standard DW-MRI of brain, since $0 \leq \delta \leq \Delta$ is required for any Stejskal-Tanner sequence, Δ is typically in the range of 20 to 200 ms, and R_e in brain has been estimated to be roughly 10 s^{-1} [21]. We note that ε is independent of the diffusivities and the number fractions, as these enter the ADK only through the prefactor K_0 in Eq. (23).

A contour plot for ε is shown in Fig. 1. The error vanishes for either $\delta / \Delta = 0$, in accord with Eq. (10), or for the no exchange limit of $R_e\Delta = 0$. The error also vanishes for a line corresponding approximately to$\delta / \Delta = 0.85$; to the left of this line, the error is positive, while to the right it is negative. The maximum amplitude of the error is 6.2% for $\delta / \Delta = 0.464$ and $R_e\Delta = 6.82$. As a specific example, Fig. 2 compares $K(\Delta) / K_0$ with $K_{\text{app}}(\Delta,\delta) / K_0$ for $\delta / \Delta = 0.6$ and $R_e = 10$ s^{-1}. In this case, a maximum error of 5.63% occurs for $\Delta = 653$ms.

4. Discussion

For clinical DW-MRI, hardware and time constraints substantially limit the diffusion information that is feasible to acquire. In most cases, only the ADC in selected directions and related quantities such as the diffusion tensor eigenvalues and the fractional anisotropy are estimated.

Recent work has demonstrated that the diffusional kurtosis may also be obtained using clinical scanners within scan times of a few minutes, thus adding a new diffusion metric to the clinical toolbox [4–7]. The practical estimation of the kurtosis is based of the formula

$$\ln\left(\frac{S(b)}{S(0)}\right) = -bD_{\text{app}} + \frac{1}{6}b^2 D_{\text{app}}^2 K_{\text{app}} + O(b^3), \tag{25}$$

where $S(b)$ is the signal amplitude as a function of the b-value. Fitting $\ln[S(b)]$ data for three or more b-values to Eq. (25), with the $O(b^3)$ terms excluded, then yields estimates for both the ADC and the ADK. This procedure is a simple extension of the conventional linear fit to $\ln[S(b)]$ used in diffusion tensor imaging. In brain, fits to Eq. (25) usually employ maximum b-values of about 2000 to 3000 s/mm^2. In practice, the accuracy of estimates for the ADC and ADK may depend on a variety of factors including the signal-to-noise ratio, choice of b-values, and intrinsic tissue properties such as inter-compartmental water exchange rates [6].

One potential confounding effect stems from the fact that the gradient pulse durations for clinical DW-MRI are typically long because of hardware limitations, often being

comparable to the diffusion time Δ [1]. For this reason, the narrow pulse limit connections of Eqs. (7) and (10), for the ADC and ADK to the ideal diffusion coefficient and kurtosis, do not necessarily apply. Moreover, a strong dependence of the ADC and ADK on pulse duration would make them less attractive as clinical measures, since their values would depend significantly on the specific sequence parameters utilized.

However, a prior theoretical study of diffusion in open geometries [3] and an experimental study of water diffusion in rat thalamus [17] have both found the effect of pulse duration on the ADC to be relatively small. These results therefore help to justify use of the ADC for clinical applications.

Here we have performed a similar theoretical analysis for the KM ADK, finding that an extended pulse duration changes the ADK by at most a few percent for model parameters relevant to DW-MRI of brain. Although not definitive, our results do suggest that the water ADK in brain is insensitive to changes in the pulse duration, supporting the robustness of ADK estimates based on clinical DW-MRI. The previously mentioned rat thalamus experimental study also observed the water ADK to change very little with pulse duration [17], in consistency with our findings.

Acknowledgments

This work was supported in part by NIH grants R01AG027852 and R01EB007656, as well as by the Litwin Foundation for Alzheimer's Research.

References

1. Basser PJ. Relationships between diffusion tensor and q-space MRI. Magn Reson Med. 2002; 47:392–397. [PubMed: 11810685]
2. Wang LZ, Caprihan A, Fukushima E. The narrow-pulse criterion for pulsed-gradient spin-echo diffusion measurements. J Magn Reson A. 1995; 117:209–219.
3. Zielinski LJ, Sen PN. Effects of finite-width pulses in the pulsed-field gradient measurement of the diffusion coefficient in connected porous media. J Magn Reson. 2003; 165:153–161. [PubMed: 14568525]
4. Jensen JH, Helpern JA, Ramani A, Lu H, Kaczynski K. Diffusional kurtosis imaging: the quantification of non-Gaussian water diffusion by means of magnetic resonance imaging. Magn Reson Med. 2005; 53:1432–1440. [PubMed: 15906300]
5. Lu H, Jensen JH, Ramani A, Helpern JA. Three-dimensional characterization of non-Gaussian water diffusion in humans using diffusion kurtosis imaging. NMR Biomed. 2006; 19:236–247. [PubMed: 16521095]
6. Jensen JH, Helpern JA. MRI quantification of non-Gaussian water diffusion by kurtosis analysis. NMR Biomed. 2010; 23:698–710. [PubMed: 20632416]
7. Poot DH, den Dekker AJ, Achten E, Verhoye M, Sijbers J. Optimal experimental design for diffusion kurtosis imaging. IEEE Trans Med Imaging. 2010; 29:819–829. [PubMed: 20199917]
8. Lazar M, Jensen JH, Xuan L, Helpern JA. Estimation of the orientation distribution function from diffusional kurtosis imaging. Magn Reson Med. 2008; 60:774–781. [PubMed: 18816827]
9. Falangola MF, Jensen JH, Babb JS, Hu C, Castellanos FX, Di Martino A, Ferris SH, Helpern JA. Age-related non-Gaussian diffusion patterns in the prefrontal brain. J Magn Reson Imaging. 2008; 28:1345–1350. [PubMed: 19025941]
10. Hui ES, Cheung MM, Qi L, Wu EX. Towards better MR characterization of neural tissues using directional diffusion kurtosis analysis. Neuroimage. 2008; 42:122–134. [PubMed: 18524628]
11. Cheung MM, Hui ES, Chan KC, Helpern JA, Qi L, Wu EX. Does diffusion kurtosis imaging lead to better neural tissue characterization? A rodent brain maturation study. Neuroimage. 2009; 45:386–392. [PubMed: 19150655]

12. Wu EX, Cheung MM. MR diffusion kurtosis imaging for neural tissue characterization. NMR Biomed. 2010; 23:836–848. [PubMed: 20623793]
13. Raab P, Hattingen E, Franz K, Zanella FE, Lanfermann H. Cerebral gliomas: diffusional kurtosis imaging analysis of microstructural differences. Radiology. 2010; 254:876–881. [PubMed: 20089718]
14. Jansen JF, Stambuk HE, Koutcher JA, Shukla-Dave A. Non-Gaussian analysis of diffusion-weighted MR imaging in head and neck squamous cell carcinoma: a feasibility study. Am J Neuroradiol. 2010; 31:741–748. [PubMed: 20037133]
15. Jensen JH, Falangola MF, Hu C, Tabesh A, Rapalino O, Lo C, Helpern JA. Preliminary observations of increased diffusional kurtosis in human brain following recent cerebral infarction. NMR Biomed. Published online ahead of print Oct. 19, 2010.
16. Helpern JA, Adisetiyo V, Falangola MF, Hu C, Di Martino A, Williams K, Castellanos FX, Jensen JH. Preliminary evidence of altered gray and white matter microstructural development in the frontal lobe of adolescents with ADHD: a diffusional kurtosis imaging study. J Magn Reson Imaging. 2011; 33:17–23. [PubMed: 21182116]
17. Minati L, Zucca I, Carcassola G, Occhipinti M, Spreafico R, Bruzzone MG. Effect of diffusion-sensitizing gradient timings on the exponential, biexponential and diffusional kurtosis model parameters: in-vivo measurements in the rat thalamus. Magn Reson Mater Phys. 2010; 23:115–121.
18. Kärger J. NMR self-diffusion studies in heterogeneous systems. Adv Colloid Interface Sci. 1985; 23:129–148.
19. Kärger J, Pfeifer H, Heink W. Principles and applications of self-diffusion measurements by nuclear magnetic resonance. Adv Magn Reson. 1988; 12:1–89.
20. Stanisz GJ, Szafer A, Wright GA, Henkelman RM. An analytical model of restricted diffusion in bovine optic nerve. Magn Reson Med. 1997; 37:103–111. [PubMed: 8978638]
21. Lee JH, Springer CS Jr. Effects of equilibrium exchange on diffusion-weighted NMR signals: the diffusigraphic “shutter-speed”. Magn Reson Med. 2003; 49:450–458. [PubMed: 12594747]
22. Nilsson M, Lätt J, Nordh E, Wirestam R, Ståhlberg F, Brockstedt S. On the effects of a varied diffusion time in vivo: is the diffusion in white matter restricted? Magn Reson Imaging. 2009; 27:176–187. [PubMed: 18657924]
23. Fieremans E, Novikov DS, Jensen JH, Helpern JA. Monte Carlo study of a two-compartment exchange model of diffusion. NMR Biomed. 2010; 23:711–724. [PubMed: 20882537]
24. Meier C, Dreher W, Leibfritz D. Diffusion in compartmental systems. I. A comparison of an analytical model with simulations. Magn Reson Med. 2003; 50:500–509. [PubMed: 12939757]
25. Roth Y, Ocherashvilli A, Daniels D, Ruiz-Cabello J, Maier SE, Orenstein A, Mardor Y. Quantification of water compartmentation in cell suspensions by diffusion-weighted and T_2-weighted MRI. Magn Reson Imaging. 2008; 26:88–102. [PubMed: 17574364]
26. Jensen JH, Chandra R. Weak-diffusion theory of NMR signal in magnetically heterogeneous media. J Magn Reson. 1997; 126:193–199.
27. Stejskal EO, Tanner JE. Spin diffusion measurements: spin echoes in the presence of a time-dependent field gradient. J Chem Phys. 1965; 42:288–292.
28. Tanner JE, Stejskal EO. Restricted self-diffusion of protons in colloidal systems by the pulsed-gradient, spin-echo method. J Chem Phys. 1968; 49:1768–1777.
29. van Kampen NG. Derivation of the phenomenological equations from the master equation: 1. even variables only. Physica. 1957; 23:707–719.
30. de Groot SR, Mazur P. On the statistical basis of Onsager’s reciprocal relations. Physica. 1957; 23:73–81.
31. Cao J. Single molecule tracking of heterogeneous diffusion. Phys Rev E. 2001; 63:041101-1–041101-7.

5. Appendix

In order to derive Eqs. (16) and (18), it is convenient to introduce the displacement probability density, $P_{ij}(x,t)$, which corresponds to the solution of Eq. (11) with the initial condition

$$P_{ij}(x,0)=\delta_{ij}\delta(x). \tag{26}$$

Physically, $P_{ij}(x,t)$ is the probability density for moving a distance x over a time interval t, while beginning in compartment j and ending in compartment i. Given the probability density, the particle concentration is determined by

$$C_i(x,t)=\sum_{j=1}^{N}\int_{-\infty}^{\infty} dy P_{ij}(x-y,t)C_j(y,0), \tag{27}$$

so that $P_{ij}(x,t)$ plays the role a Green's function for Eq. (11).

If we define Fourier transformed probability $\tilde{P}_{ij}(q,t)$ by

$$P_{ij}(x,t)=\int_{-\infty}^{\infty}\frac{dq}{2\pi}\tilde{P}_{ij}(q,t)e^{iqx}, \tag{28}$$

then the KM equations can be rewritten as

$$\frac{\partial}{\partial t}\tilde{P}_{ij}(q,t)=-D_i q^2\tilde{P}_{ij}(q,t)+\sum_{k=1}^{N}R_{ik}\tilde{P}_{kj}(q,t), \tag{29}$$

with the initial condition

$$\tilde{P}_{ij}(q,0)=\delta_{ij}. \tag{30}$$

Here the parameter q is analogous to the wavenumber of q-space MRI [1].

By applying standard methods, one can obtain the solution

$$\tilde{P}_{ij}(q,t)=\sqrt{\frac{f_i}{f_j}}\sum_{n=1}^{N}\alpha_{i,n}(q)\alpha_{j,n}(q)e^{-\lambda_n(q)t}. \tag{31}$$

Here $\alpha_{i,n}(q)$ indicates a complete set of N orthonormal eigenvectors with the eigenvalues $\lambda_n(q)$ so that

$$\lambda_n(q)\alpha_{i,n}(q)=D_i q^2\alpha_{i,n}(q)-\sum_{j=1}^{N}R_{ij}\sqrt{\frac{f_j}{f_i}}\alpha_{j,n}(q). \tag{32}$$

Note that $\alpha_{i,n}(q)$ and $\lambda_n(q)$ are even functions of q and that $\lambda_n(q) \geq 0$ for any physically sensible solution. The completeness and orthogonality of $\alpha_{i,n}(q)$ follow from the fact that they are the eigenvectors of a real symmetric matrix, which is a consequence of the detailed balance condition of Eq. (15).

In terms of the displacement probability, the second order position correlation function can be written

$$\langle x(t_1)x(t_2)\rangle=\sum_{i,j,k=1}^{N}\int_{-\infty}^{\infty}x_2dx_2\int_{-\infty}^{\infty}x_1dx_1P_{ij}(x_2-x_1,t_2-t_1)P_{jk}(x_1,t_1)f_k, \tag{33}$$

for $t_1 \leq t_2$. By using Eq. (28), this can be reduced to

$$\langle x(t_1)x(t_2)\rangle=-\sum_{i,j=1}^{N}\left[\frac{\partial^2}{\partial^2 q}\tilde{P}_{ij}(q,t_1)f_j\right]\Big|_{q=0}. \tag{34}$$

An analogous argument for the fourth order position correlation function leads to

$$\langle x(t_1)x(t_2)x(t_3)x(t_4)\rangle=\sum_{i,j,k,l=1}^{N}\left[\left(\frac{\partial^4}{\partial^4 q_1}+3\frac{\partial^2}{\partial^2 q_1}\frac{\partial^2}{\partial^2 q_2}+\frac{\partial^2}{\partial^2 q_1}\frac{\partial^2}{\partial^2 q_3}\right)\tilde{P}_{ij}(q_3,t_3-t_2)\times\tilde{P}_{jk}(q_2,t_2-t_1)\tilde{P}_{kl}(q_1,t_1)f_l\right]\Big|_{q_1,q_2,q_3=0}, \tag{35}$$

where $t_1 \leq t_2 \leq t_3 \leq t_4$.

For the special case of $N = 2$, the transition rate constants may be written as the 2×2 matrix

$$\begin{pmatrix} R_{11} & R_{12} \\ R_{21} & R_{22} \end{pmatrix}=R_e\begin{pmatrix} -f_2 & f_1 \\ f_2 & -f_1 \end{pmatrix}, \tag{36}$$

which automatically satisfies the constraints of Eqs. (14) and (15).

By solving the eigenvector problem of Eq. (32) for $N = 2$, one finds the KM eigenvalues to be

$$\lambda_1=\frac{1}{2}[(D_1+D_2)q^2+R_e]-\frac{1}{2}\sqrt{(D_1-D_2)^2q^4-2R_e(f_1-f_2)(D_1-D_2)q^2+R_e^2} \tag{37}$$

and

$$\lambda_2=\frac{1}{2}[(D_1+D_2)q^2+R_e]+\frac{1}{2}\sqrt{(D_1-D_2)^2q^4-2R_e(f_1-f_2)(D_1-D_2)q^2+R_e^2}. \tag{38}$$

The corresponding eigenvectors are

$$\alpha_{i,1}=\frac{1}{\sqrt{1+c^2}}\begin{pmatrix}1\\ c\end{pmatrix};\quad \alpha_{i,2}=\frac{1}{\sqrt{1+c^2}}\begin{pmatrix}-c\\ 1\end{pmatrix}, \tag{39}$$

where

$$c=\frac{D_1q^2+R_ef_2-\lambda_1}{R_e\sqrt{f_1f_2}}. \tag{40}$$

A straightforward, albeit lengthy, calculation using Eqs. (31) and (34)–(40) leads then directly to the results of Eqs. (16) and (18).

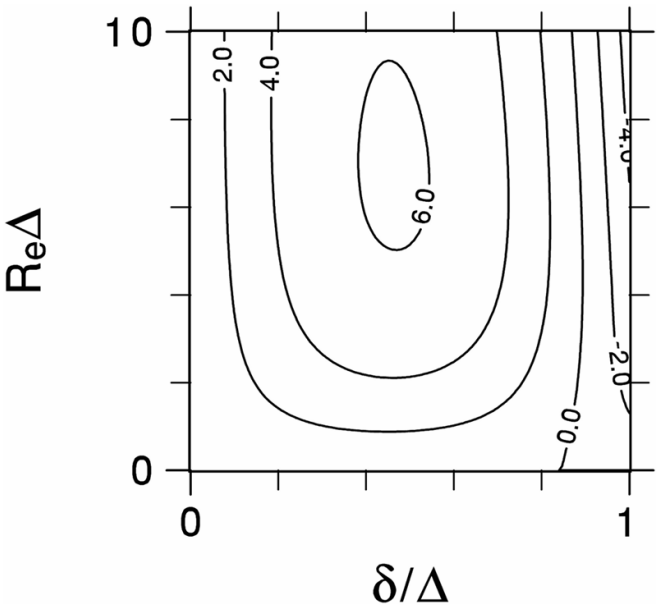

Fig 1.

Contour plot of the percent error for the apparent diffusional kurtosis as calculated with the Kärger model and a Stejskal-Tanner pulse sequence.

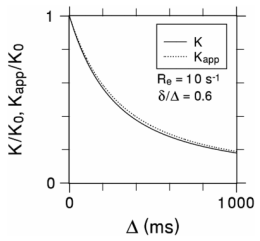

Fig 2.

True (K) and apparent (K_{app}) diffusional kurtoses as functions of the diffusion time for R_e = 10 s^{-1} and δ/Δ = 0.6. The two curves nearly coincide demonstrating the insensitivity of K_{app} to the gradient pulse duration.